AERODYNAMIC EFFICIENCY STUDY UNDER THE INFLUENCE OF HEAVY RAIN VIA TWO-PHASE FLOW APPROACH

Tung Wan, Szu-Peng Pan
Department of Aerospace Engineering, Tamkang University
Tamsui, Taipei County, Taiwan, 251, Republic of China

Keywords: ***heavy rain, two phase flow***

Abstract

The detrimental effects of some meteorological phenomenon such as wind shear, thunderstorm, ice/snow etc, to aviation safety are relatively well known. But aerodynamic influences due to heavy rain are still an on-going research subject, and needs further investigation. In the past decade there are neither experimental nor numerical researches on heavy rain aerodynamics except our numerical simulation conducted at 2003. This paper first review some research finding of heavy rain effects on aerodynamic performance degradation. To further investigate the rain physics, CFD method and preprocessing grid generator are used as our main analytical tools, and the simulation of rain is accomplished via two-phase flow approach's Discrete Phase Model (DPM). The current discoveries of a typical commercial airfoil show that this research successfully simulates the low speed aerodynamic efficiency degradation under the heavy rain. The degradation rate increases with the rain rate, and the premature stall phenomenon is also reported. It is expected that the quantitative information gained in this paper will be useful to the operational airline industry, and greater effort such as flight test should put in this direction to further improve aviation safety.

1 Introduction

Recently global warming phenomenon has aroused public's attention and being widely discussed. It is stated that the direct influences of global warming are the changes of weather behavior and, more important, the occurrences of severe weather. It is clear that weather influences everyone's daily life more and more. Weather has always played an important role in aviation safety; weather phenomena that hazard flight safety include low level wind shear, gust wind, clear air turbulence (CAT), ice, frost, heavy rain, fog, typhoon, tornado, thunderstorm, lighting, etc. A review of aircraft accident records in the past decades clearly shows the necessity of aircraft avoiding the most severe weather environments, such as those associated with thunderstorms.

On August 22, 1979, Eastern Airlines Flight 693, a Boeing 727-25, encountered a small but intense rain shower coupled with wind shears during final approach to the Atlanta International Airport. The aircraft came within 375 ft of crashing before it exited the shower and a terrifying missed approach was completed [1]. In Taiwan, there are also numerous accidents related to heavy rains. For instance, on July 14, 2006, a MD-80 transport of Far Eastern Air flight 066 encountered a heavy rain shower and unstable wind while preceding the landing approach. It is confirmed that after touchdown the aircraft run into grass field beside runway for a short period of time, and cause severe damage to the main landing gear.

As the two cases stated above, the adverse weather can be a hazardous factor to aircraft, especially during take-off and landing phases, for aircraft operating at this stage is at relatively low altitude and low speed. The flight manuals for all commercial airlines clearly warn the pilots to avoid the vicinity of a thunderstorm and to penetrating any thunderstorm cells. The occurrence of thunderstorm is always accompanied by heavy rain shower and gust wind. While the danger of wind shear has been fully investigated and understood, but the detrimental effect of heavy rain is generally believed to be low comparing to wind shear effect, so the studies of heavy rain influence on the airfoil has long been ignored and not widely discussed.

Although there have been some experimental research to analyze the aerodynamic efficiency penalties under heavy rain, there still some limited progress in numerical simulation. In 1994 and 1995, Valentine and Decker [2][3][4], conducted a series numerical simulation to investigate the airfoil performance under heavy rain. Their research successfully simulates rain phenomenon, and the degradation of aerodynamic efficiency is also achieved. However, detailed physics of rain still lacking in their research, and further verification of their results need to be investigated and compared. In 2003, Wan and Wu also conducted the numerical simulation of heavy rain effect on airfoil [5]. The main focus of that work is to add the water film layer and vertical rain mass flow rate on the airfoil upper surface, thus increasing the airfoil roughening effects. Now in this work we try to employ a new two-phase flow approach to the same problem, adding more rain mechanical behavior to the airfoil, and compare with the experimental results done earlier.

2 Research Background

The first study of heavy rain effects on aircraft flight was performed by Rhode in 1941 [6]. He concluded that the most severe performance penalty experienced by DC-3 aircraft flying through a rainstorm with Liquid Water Content (LWC) of 50 g/m^3 was due to the loss of aircraft momentum caused by collisions with raindrops. It was estimated that this effect could result in a decrease in airspeed of up to 18 percent, but the duration of the rain would not be sufficient to pose a significant threat to an aircraft at cruising altitude of 5000 ft. Rhode recognized that the surface of the aircraft may be effectively roughened by rain but noted that insufficient test data existed to evaluated this effect.

In 1987, Hansman examined the performance of a small-scale wind-tunnel laminar flow test of Wortmann FX67-K170, NACA0012, and NACA64-210 airfoils [7]. The simulated rain rate is 1000 mm/h and Reynolds number of 3.1×10^5, lift and drag were measured in both dry and wet conditions. At low angles of attack, the lift degradation in wet conditions varied significantly between the airfoils. The Wortman section had the greatest lift degradation (~25%) and the NACA64-210 airfoil had the least (~5%). At high angles of attack, the NACA64-210 and NACA0012 airfoils were observed to even have improved aerodynamic in rain conditions due to a reduction of boundary-layer separation. Once the dominated laminar flow on the dry airfoil was tripped to turbulence; the original flow separation behavior of laminar flow has been improved.

At the same time, NASA and the FAA developed a large-scale, ground-based test capability at the Langley Aircraft Landing Dynamics Facility (ALDF) led by Bezos to assess the effect of rain on airfoil performance at more realistic Reynolds number [8]. The NACA64-210 airfoil section was choose to be the tested wing and had a 10 ft chord and 13.1 ft span. An over head rain simulation system was constructed along a 525 ft section of the track. The system produced realistic rainfall intensities of 2, 10, 30, and 40 in/hr (corresponding to LWC=2, 9, 26, and 35 g/m^3) that were consistent with airborne and ground-based rain fall data measured in convective rainstorm. This outdoor, full-scale experiment is conducted due to the scaling difficulties of droplets diameters for extrapolation of subscale data to full scale conditions. In that study, the lift slope degradation has been revealed, and drag slope also increased with the rain rate increase.

In 1995, Valentine and Decker conducted numerical simulation of heavy rain effects on NACA64-210 airfoil. To assess the airfoil performance in rain, a two-way momentum coupled, two-phase flow scheme was deployed for the evaluation of the effect of splashed-back droplets on the airfoil. Non-interacting, non-deforming, and non-evaporating spherical particles representing statistical distributions of raindrops are tracked through the curvilinear body-fitted grid. A Lagrangian particle tracking algorithm has been used and linked with a thin layer incompressible Navier-Stokes code. In that research, two physical phenomena have been hypothesized to be responsible for the degradation of airfoil performance in rain, the loss of boundary layer momentum to splashed back droplets and the effective roughening of the airfoil surface due to an uneven water film [4]. Their numerical results show a more severe rain induced stall but no change in airfoil performance until a stall angle is reached.

In 2003, Wan and Wu investigated the same issue and conducted the numerical simulation of heavy rain effects on airfoil. The primary objective is to establish the thickness of water film on airfoil, and to simulate the airfoil roughening effects. Also they try to estimate the aerodynamics changed by rainfall mass flow rate. These properties include density, pressure, velocity, and angle of attack. They combined all these factors and implement the Navier-Stokes flow solver coupled with a Bowyer's type unstructured grid system. There are total 7 cases have been investigated, with different airspeeds, airfoil shapes, and rain rates. The results indicate that at low Mach number with LWC=30 g/m^3, the lift coefficient decrease about 7.3% and drag coefficient increase about 38% [5]. Compare with NASA's experimental data at the same Reynolds number, some difference are still being observed.

In experimental or numerical simulation, rainfall's intensity often measured in terms of Liquid Water Content (LWC) of the air or the mass of the water per unit volume of air. The relation between rainfall rate (R, mm/h) to LWC (g/m^3) is determined to be

$$LWC=0.054R^{0.84}$$

Subsequently, we should determine the rain droplet speed when impacting the airfoil. Hence, calculating the terminal velocity of each rain droplet is essential for our investigation. The meaning of terminal velocity is that during the process of a free fall, the falling object is maintaining a constant speed and is not accelerating. The reason is that frictional drag force due to air and the gravity force of the object are in equilibrium condition. The same physical explanation can apply to the rain droplets. It is assumed that when aircraft go through a severe thunderstorm during take-off or landing, the large raindrops must created at a relatively mid or higher altitude, thus later near the ground surface will fall with the terminal velocities. The terminal velocity of a raindrop is a function of droplet size and altitude and has been established by Marlowitz as

$$V_T(m/s)=9.58\left\{1-\exp\left[-\left(\frac{d(mm)}{1.77}\right)^{1.147}\right]\right\}$$

where V_T is the terminal velocity, and the d is the rain droplet size in mm [10]. Several mechanisms have been hypothesized as contributing to the degradation of airfoil (or aircraft) performance in heavy rain. They can be categories as follows:

(a)The loss of aircraft momentum due to collisions with raindrops,

(b)The effective roughening of the airfoil surface due to the presence of an uneven water layer,

(c)The loss of boundary layer air momentum due to splash back of droplets into the airflow field as raindrops strike the airfoil surface.

As raindrops strike on airfoil, an "ejecta fog" of splashed-back droplets forms at the leading edge. For numerical simulation, this phenomenon has been hypothesized that the acceleration of these droplets in the boundary layer by the airflow field may act as a momentum sink for the boundary layer, resulting in a decreased airflow velocity. Deceleration of the boundary layer can lead to a loss of lift, premature separation and stall, and increase in drag.

Beneath the ejecta fog layer, a thin water film forms on the airfoil surface because of the fraction of the raindrop that is not splashed back. The thickness of the water film has been measured in small-scale wind tunnel investigation to be of the order of 0.1 mm or less and has been estimated at full scale to be about 1 mm or less. Raindrop impact "craters" and surface waves in the water film effectively roughen the airfoil surface. The adverse effect of this rougher surface upon aerodynamic performance has been analyzed in detail by Haines and Luers [12]. As the water film is carried downstream, rivulets form on the back portion of the airfoil. With increasing angle of attack, the extent of the water film decreases on the upper surface and increase on the lower surface. When stall is reached, this rivulet disappears and pooling of water occurs on the separated portion of the airfoil.

From the above descriptions we know that heavy rain effect on airfoil is an important but complicated process, but only two numerical simulation works have been done so far. So current research plan is to implement the newest two-phase flow technique and combine with our past experience to unravel the rain's degradation effect at Reynolds number of 3.0×10^6.

3 Numerical Modeling

In this research, the creating of geometry and generating of grid are both achieved by software. Gambit can generate different meshes types, such as structured, multi-block, unstructured, or hybrid grids. Here the airfoil shape is choosing as NACA64-210, which is used for many modern transport aircraft wing section. Due to the simple geometry, structure type grid is adopted for the mesh system. The advantage of structure grid is not only save the numbers of grids, it also can predict more accurate flow behaviors at wall boundary. The mesh constructed in the work is shown below, the chord length is 3.048 m, and the numbers of cell is 10400.

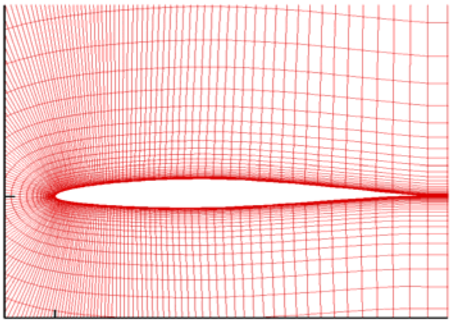

Figure 1 Near mesh of NACA 64-210 airfoil

For Reynolds number 3.0×10^{6}, the flow behavior is characterized as turbulent, thus adding turbulence model to governing equation is an important part of our simulation. The Reynolds-averaged Navier-Stokes (RANS) equations represent transport equations for the mean flow only; with all turbulent scales have been modeled. This approach of permitting a solution for mean flow variables greatly reduces the computational effort. With the Boussinesq hypothesis, this Reynolds-averaged approach is adopted for many practical engineering calculations, and the Spalart-Allmaras and κ-ε models are chosen as our turbulence model candidates.

In our investigation, FLUENT is used to solve conservation equations of mass, momentum and energy of the flow field after discretization with finite volume method. It supplies two kinds of solvers to solve the properties: pressure-based solver and density-based solver. In the pressure-based solver, the constraint of mass conservation (continuity) of the velocity field is achieved by solving a pressure (or pressure correction) equation. The pressure equation is derived from the continuity and the momentum equations in such a way that the velocity field, corrected by the pressure, satisfies the continuity. Since the governing equations are nonlinear and coupled to one another, the solution process involves iterations wherein the entire set of governing equations is solved repeatedly until the solution converges.

Two pressure-based solver algorithms are available in FLUENT: a segregated algorithm, and a coupled algorithm [13]. In the segregated algorithm, the individual governing equations for the solution variables are solved one after another. Each governing equation, while being solved, is "decoupled" or "segregated" from other equations. The segregated algorithm is memory-efficient, since the discretized equations need only be stored in the memory one at a time. However, the solution convergence is relatively slow, in as much as the equations are solved in a decoupled manner.

FLUENT provides four segregated types of algorithms: SIMPLE, SIMPLEC, PISO, and (for time-dependant flows using the Non-Iterative Time Advancement option (NITA)) Fractional Step (FSM). These schemes are referred to as the pressure-based segregated algorithm. Steady-state calculations will generally use SIMPLE or SIMPLEC, while PISO is recommended for transient calculations. In this study, the boundary condition is set to velocity inlet. For incompressible flow, the density is set to constant. During the calculation of rain condition, the time is discretized in first order implicit and use the QUICK scheme in momentum discretization. Finally, the SIMPLE algorithm is implemented to discretize the velocity-pressure coupling term.

3.1 Multi-Phase Flow Approach

In the natural world, a large number of flow conditions are in the form of mixture phases. Advances in computational fluid mechanics have provided the basis for further insight into the dynamics of multiphase flows. Currently there are two approaches for the numerical calculation of multiphase flows: the Eulerian-Lagrangian approach and the Eulerian-Eulerian approach. In the Eulerian-Eulerian approach, the different phases are treated mathematically as interpenetrating continua. Since the volume of a phase cannot be occupied by the other phases, the concept of phase volume fraction is introduced. These volume fractions are assumed to be continuous functions of space and time and their sum is equal to one.

In Eulerian-Lagrangian approach, the fluid phase is treated as a continuum by solving the time-averaged Navier-Stokes equations, while the dispersed phase is solved by tracking a large number of particles, bubbles, or droplets through the calculated flow field. The dispersed phase can exchange momentum, mass, and energy with the fluid phase. In addition to solving transport equations for the continuous phase, we can simulate a discrete second phase in a Lagrangian reference frame. This model is called Discrete Phase Model (DPM). This second phase consists of spherical particles (which may be taken to represent droplets or bubbles) dispersed in the continuous phase. The trajectories of these discrete phase entities are computed, as well as heat and mass transfer to/from them. The coupling between the phases and its impact on both the discrete phase trajectories and the continuous phase flow can be included.

We can predict the trajectory of a discrete phase particle (or droplet or bubble) by integrating the force balance on the particle, which is written in a Lagrangian reference frame. This force balance equates the particle inertia with the forces acting on the particle, and can be written (for the x direction in Cartesian coordinates) as

$$\frac{du_p}{dt} = F_D(u-u_p) + \frac{g_x(\rho_p-\rho)}{\rho_p} + F_x \qquad (1)$$

where F_x is an additional acceleration (force/unit particle mass) term, $F_D(u-u_p)$ is the drag force per unit particle mass and

$$F_D = \frac{18\mu}{\rho_p d_p^2}\frac{C_D \mathrm{Re}}{24} \qquad (2)$$

Here, u is the fluid phase velocity, u_p is the particle velocity, μ is the molecular viscosity of the fluid, ρ is the fluid density, ρ_p is the density of the particle, and d_p is the particle diameter. Re is the relative Reynolds number, which is defined as

$$\mathrm{Re} = \frac{\rho d_p |u_p - u|}{\mu} \qquad (3)$$

In order to construct rain injection, first we establish the rain injection control volume. For DPM input parameters, it needs to input the mass flow (kg/m^3) rate for every injection point. Assume the injection area is 42m×1m (1m is the unit length), and the free stream velocity is 12.4603 m/s, thus we can obtain the volume flow rate is 523.3341 m^3/s. For rain condition, assume the rain rate is at LWC=39 g/m^3. According the volume flow rate obtained above, we can acquire the mass flow rate is 20410.02925 g/m^3 or 20.41 kg/s From statistic table from previous research, the distance between each droplet particle is 7 cm, thus we can acquire the droplet number as 600 Hence, the mass flow rate for each point 0.03402 kg/s.

In order to simulate the rain phenomenon in this thesis, the DPM model is employed, and the wall film model is also activated to model the water film on the airfoil, that is, the roughening effect. Finally, the two-way coupling between discrete phase and continuous phase is used. It is expected to simulate more realistic rain behavior on the airfoil, so that the more accurate aerodynamic efficiency under heavy rain can be revealed. Papers are accepted on the basis that they may be edited for style and language. The author himself is responsible for the correctness of the scientific content.

Abbreviations should be spelt out in full the first time they appear and their abbreviated form included in brackets immediately after. Words used in a special context should appear between single quotation marks the first time they appear.

3.2 Verification

For numerical simulation, the accuracy of computational results should be validated first. The approach to achieve this verification is through the comparison of lift and drag coefficient between experimental data and numerical results. The data used as the benchmark is from Theory of Wing Section. In order to obtain the best simulation results of lift and drag coefficient, several different turbulence model are tested. Spalart-Allmaras model and κ-ε model are tested.

The airfoil is NACA64-210 of chord length equal to 3.048 m. The Reynolds number is set to 3.0×10^6 in order to be consistent for parameters of Theory of Wing Section [15]. In the verification, the Spalart-Allmaras turbulence model performs some non-satisfactory results at high AOA (Angle of Attack). The major cause is due to the unstable shear stress prediction at wall boundaries. Hence, the κ-ε model is choosing as major turbulence model. Fig. 2 shows the wall y plus distribution on the airfoil surface. This indicates that the y plus values locate in suitable range. In the lift coefficient agrees well with the experimental data before the stall AOA. At AOA of 13 degree, the experimental data shows that the stall phenomenon is occurred while the numerical results do not reveal this. Another result is conducted by Gong using CFDRC software [14]. Although his results are a little different from ours, the tendency is similar and still cannot predict the stall behavior. According to these two numerical simulations, it could state that before stall angle of attack, the numerical simulation can provide good lift results. However, Fig. 4 is the drag coefficients and it clearly shows the drag behavior of two numerical results are somewhat different. The drag coefficients conducted by this study is larger than the experiment while another result of drag behavior is quite unstable, but overall our results are still on the right track comparing with the experimental data.

In this research, the study is focus on the airfoil performance efficiency below AOA of 12 deg. Despite these inadequate results of prediction of stall angle of attack and the two numerical drag coefficients are not consistent with each other, the lift coefficient of numerical results obtained by this study below stall AOA provide excellent consistency and we can proceed this study base on this model.

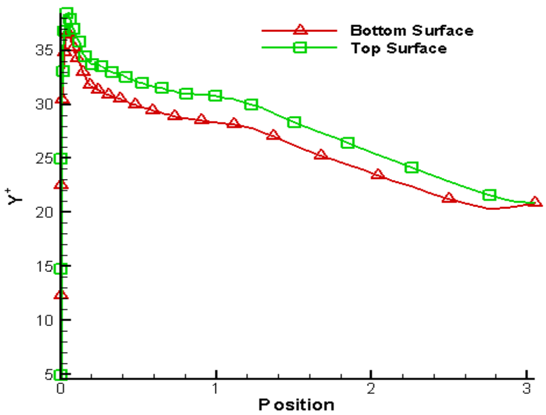

Figure 2 Wall Y plus at angle of attack 0 deg

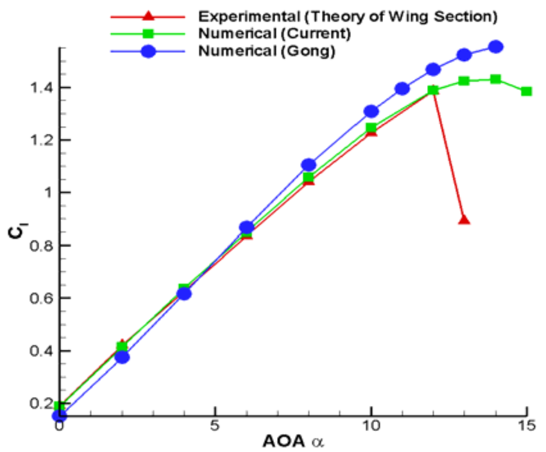

Figure 3 Lift coefficients comparison between numerical results and experiment

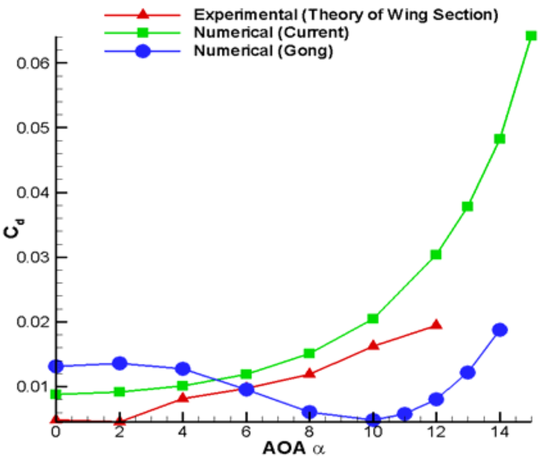

Figure 4 Drag coefficients comparison between numerical results and experiment

4 Results and Discussion

In this work, we first examine the lift and drag coefficient of no rain condition, so that the further investigation of aerodynamic performance under heavy rain can be ensured to have the right tendency. To achieve that, numerical and experimental data have acquired for comparing to the numerical results computed by this work. Fig. 5 shows the lift coefficients for different numerical simulation comparing to the experimental data. It clearly indicates that the numerical results which conducted in this work are best fitted with the data acquired by Theory of Wing Section.

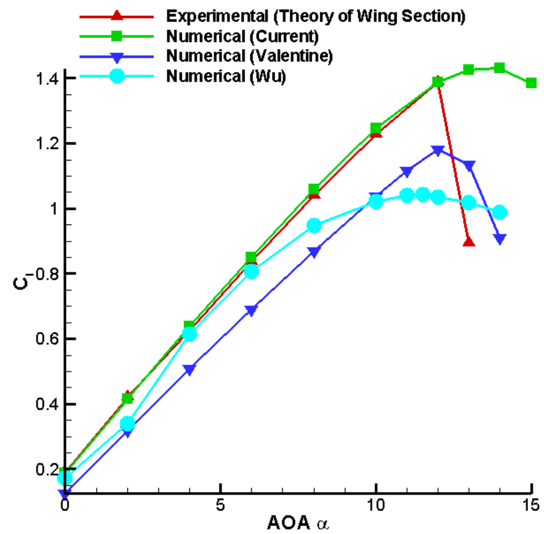

Figure 5 Lift coefficients comparison between 3 different numerical results and experiment

For the heavy rain simulation, two different rain rates are employed for investigating the rain effects to airfoil. The results are comparing to the Bezo's results, which are a large scale, outdoor, 3-D wing experiments, and then calibrate to a 2-D airfoil. Figs. 6 and 7 show the lift coefficients and drag coefficients for 3 different rain rates. Despite the inaccuracy of lift and drag prediction at stall angle of attack, the lift degradation behavior before stall angle of attack is successfully simulated. Under much heavier rain rate, the degradation is larger, the premature stall is gradually forming, and it is agree with the experimental tendencies. Moreover, the degradation rate of 2-D airfoil simulation is similar to that of the experimental data.

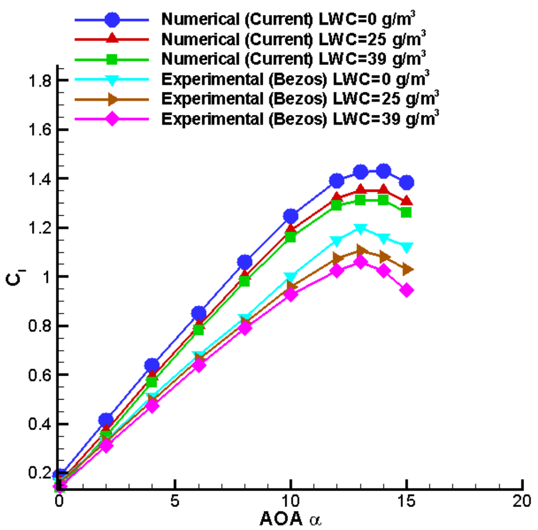

Figure 6 Lift coefficients for numerical and experimental results

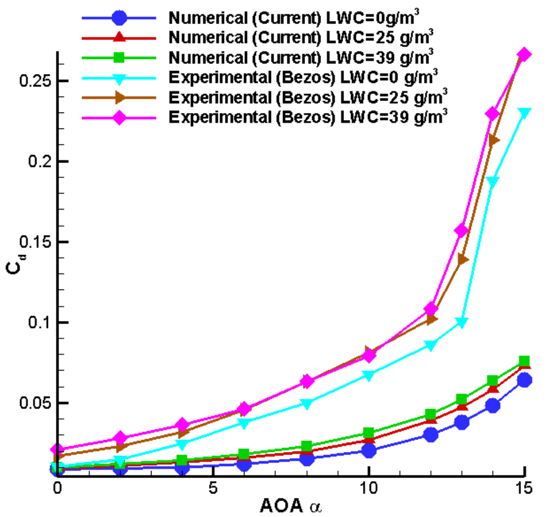

Figure 7 Drag coefficients for numerical and experimental results

The L/D of simulation and experimental data for two rain rate are more consistent. Figs. 8 and 9 are clearly indicating these tendencies. Moreover, the average L/D degradation rate for LWC=25 g/m^3 of numerical results is 25.6%, and the degradation rate of experiment is 26.6%, and at LWC=39 g/m^3, the rates of simulation and experiment are 35.2% and 34.9%. Despite the numerical results and experiment data are at different traces, their aerodynamic efficiency behavior still agrees well with each other in L/D. These surprisingly close values represent that for LWC=25 g/m^3 lighter rain rate case the aerodynamic efficiency degrades more than one-fourth of its original value; while for LWC=39 g/m^3 larger rain rate case the efficiency now degrades more than one-third of its original value. This is a fact that any civil aviation pilot cannot afford to ignore.

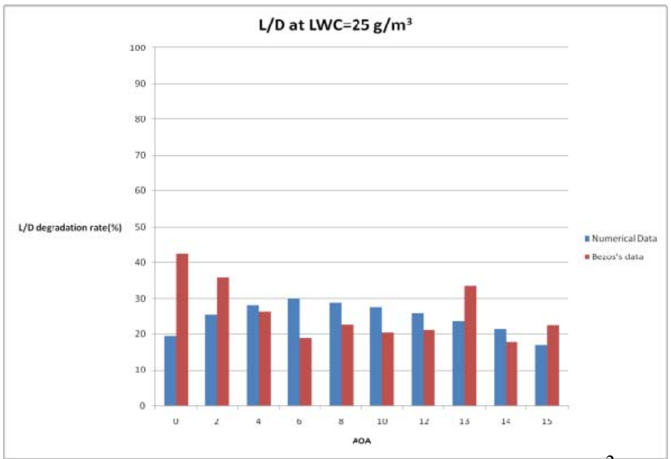

Figure 8 L/D degradation rate at LWC=25g/m^3 for numerical and experimental results

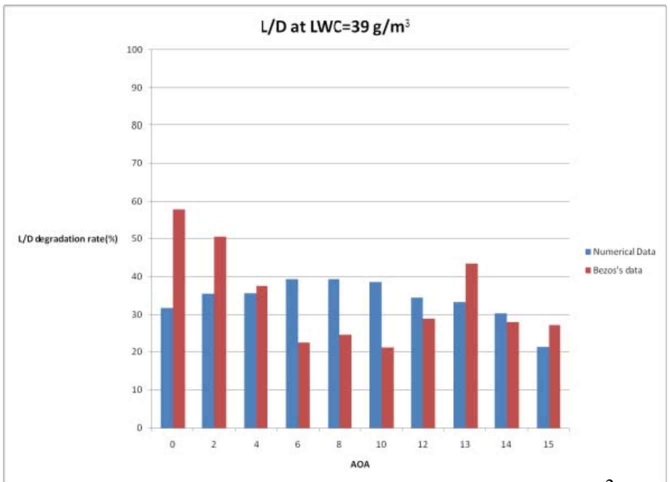

Figure 9 L/D degradation rate at LWC=39g/m^3 for numerical and experimental results

In order to explain the mechanism of our two-phase flow simulation, the following particle trace diagrams are supplied. Fig. 10 shows the global view of rain distribution in the two-phase flow computational domain, and clearly demonstrates the impact of rain droplets and wrap around the airfoil, both upper and lower surfaces.

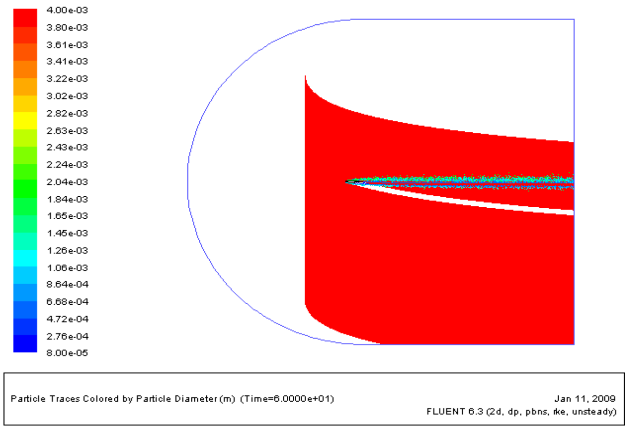

Figure 10 Global view of rain distribution

Fig. 11 and Fig. 12 show the convergence process for lifts and drag coefficients. The interesting fluctuation of the convergence is obvious. Even though, the major lift coefficient convergence tendency is still clear and the fluctuation rate is about 1 % of the average value. While this fluctuation behavior of two-phase flow on airfoil is never been reported before and may represent a numerical instability, this can also be explained by the real rain physics-droplet impact on the airfoil upper surface or the rain induced airflow fluctuation near the wall boundaries of airfoil, hence result in this phenomenon. Also, this fluctuation behavior has little effect on the overall aerodynamic efficiency factors.

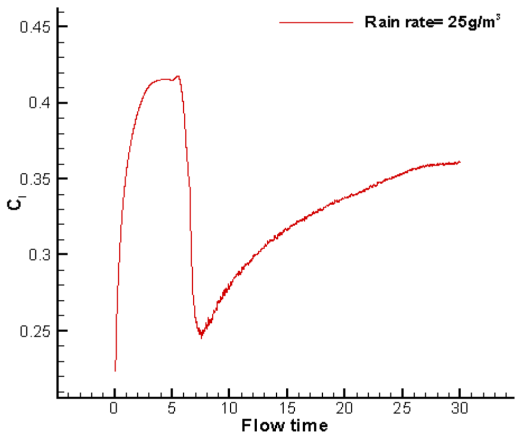

Figure 11 Lift coefficients convergence process at AOA 2 deg

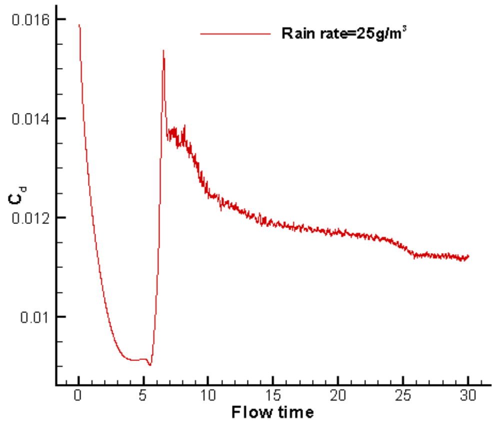

Figure 12 Drag coefficients convergence process at AOA 2 deg

Last but not least, we also simulate the NACA 64-210 airfoil with high lift devices, with configuration and unstructured grids shown in Fig. 13. Now the total grid points have increase to 51870 points. In order to make comparison with the Bezo's data, only LWC=29 g/m^3 case is considered. And we also observe the same trend in this case, namely, over-predicted in lift, but under-predicted in drag. As before, lift decrease and drag increase phenomena still exist for this high lift configuration (Figs. 14 to 15). But contrary to our intuition, now the lift decrease, drag increase, and even the lift-to-drag ratio degradation all become less in magnitude and more smoother, both in Bezos' data and our simulation. Our explanation for this is that although airfoil with high lift devices in more complicated in geometry, but through the in flux of the lower surface "clear" air blown over the upper surface of airfoil, now the heavy rain effect is becoming a little less.

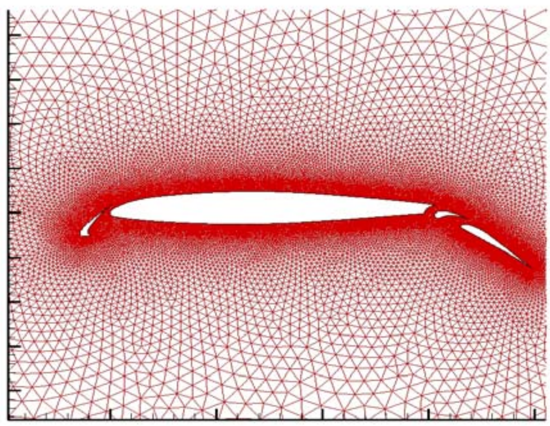

Figure 13 Near mesh of NACA 64-210 airfoil with high lift device configuration

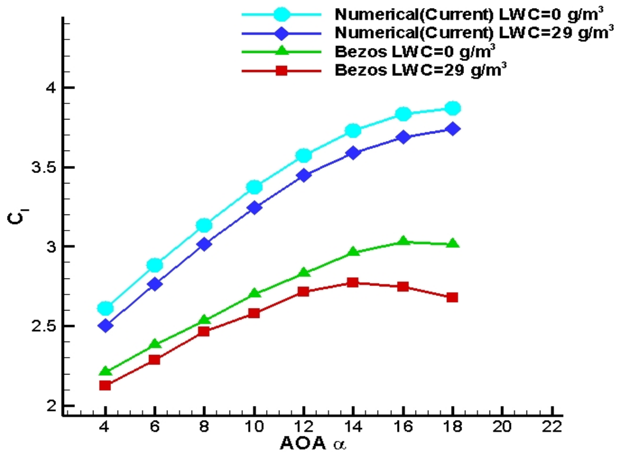

Figure 14 Lift coefficients comparison for airfoil with high lift device configuration

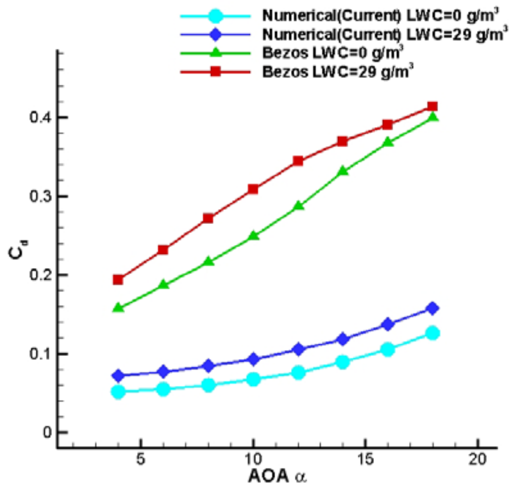

Figure 15 Drag coefficients comparison for airfoil with high lift device configuration

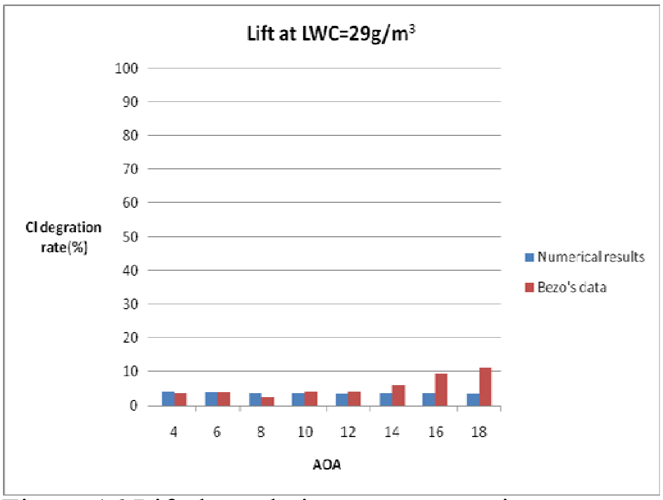

Figure 16 Lift degradation rate comparison at LWC=29g/m^3 for airfoil with high lift device configuration

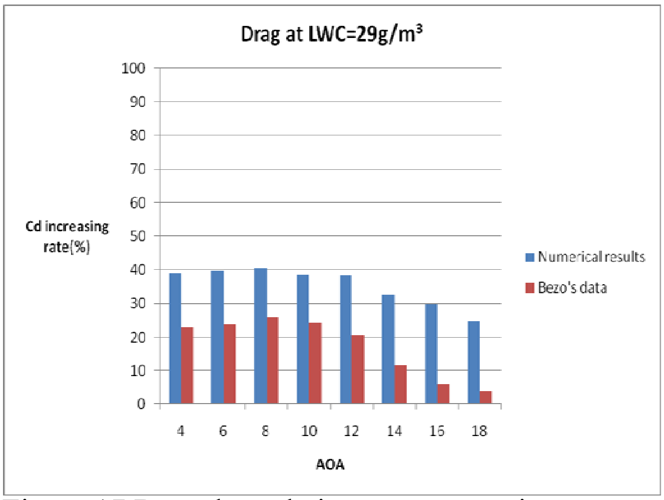

Figure 17 Drag degradation rate comparison at LWC=29g/m^3 for airfoil with high lift device configuration

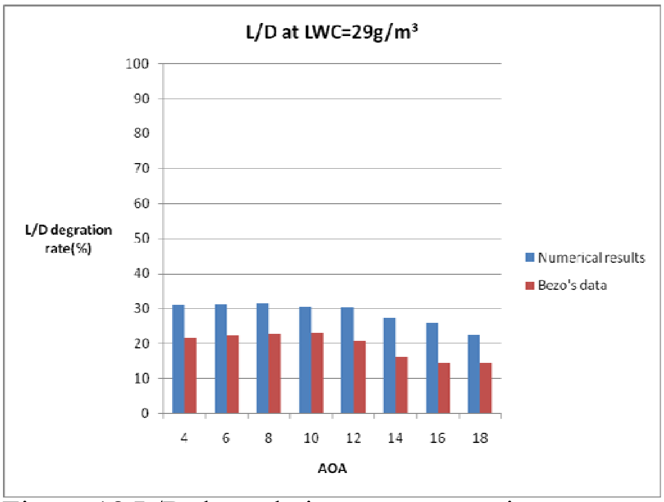

Figure 18 L/D degradation rate comparison at LWC=29g/m^3 for airfoil with high lift device configuration

As shown in the above Figs 16~18, now the lift coefficient degradation rate are all below 10 % for every angle of attack, while drag increase can come close to 40 %, especially at low angle of attack. Finally, the lift-to-drag ratio degradation is around 30 % at low AOA, and gradually decreases at high AOA. The energy draining effect of heavy rain to aircraft during take-off/landing phase is quite significant and persistent.

5 Conclusions

In summary, we could confirm that the heavy rain mechanisms established in this work can successfully simulate the aerodynamic efficiency degradation on 2-D airfoil using two-phase flow approach. In this study, the degradation rate of numerical computation is larger than the Bezos' experimental data for 25 g/m^3 and 39 g/m^3 cases respectively. And the same phenomenon is also observed for the high lift configuration, a fact never being simulated numerically before. The main reason to this phenomenon is that the differences between the original NACA data and the Bezos' experimental data. Despite this, the numerical results obtained in this work are still a good benchmark for accessing the aerodynamic performance influences for 2-D airfoil under rain conditions. Moreover, based on these 2-D numerical results, the extrapolation for 3-D wing performance degradation level under different rain rates can be a preliminary guideline for 3-D wing simulation.

The lift and drag coefficients under clean wing conditions obtained in this work have quite different tendencies compare to existing experimental data. Lift coefficients agrees well, while the drag coefficients have the minimum error percentage of 21 percent, and maximum can up to 100 percent. Although the drag prediction is not too precise, the degradation of L/D in average value is rather accurate compare with the experimental data. The drag prediction can be an issue for future investigation. It is not only for accessing the drag effect on airfoil under heavy rain, but also to improve the methodology for drag prediction of 2-D airfoil simulation. Finally, it is believed that the aerodynamic efficiency degradation rates computed in this research for different rain rates are better than expected and can be an important reference for civil aviation community.

References

[1] Luers, J. K. and Haines, P. A., "Heavy Rain Influence on Airplane Accidents," *Journal of Aircraft,* Vol. 20, No. 2, February 1983, pp. 187-191.

[2] Valentine, J. R., "Airfoil Performance in Heavy Rain," *Transportation Research Record*, No. 1428, January 1994, pp. 26-35.

[3] Valentine, J. R. and Decker, R. A., "Tracking of Raindrops in Flow over an Airfoil," *Journal of Aircraft*, Vol. 32, No. 1, Jan-Feb. 1995, pp. 100-105.

[4] Valentine, J. R. and Decker, R. A., "A Lagrangian-Eulerian Scheme for Flow around an Airfoil in Rain," *Int. J. Multiphase Flow*, Vol. 32, No. 1, 1995, pp. 639-648.

[5] Wan T. and Wu S. W., "Aerodynamic Analysis under Influence of Heavy Rain," *Journal of Aeronautics, Astronautics, and Aviation*, Nol. 41, No.3, September 2009, pp.173-180.

[6] Rhode, R. V., "Some Effects of Rainfall on Flight of Airplanes and on Instrument Indications," NACA TN903, April 1941.

[7] Hansman, R. J. Jr. and Craig, A. P., "Low Reynolds Number Tests of NACA 64-210, NACA 0012, and Wortmann FS67-K170 Airfoils in Rain," *Journal of Aircraft*, Vol. 24, No. 8, August 1987.

[8] Bezos, G. M. and Campbell, B. A., "Development of a Large-Scale, Outdoor, Ground-Based Test Capability for Evaluating the Effect of Rain on Airfoil Lift," NASA TM-4420, April 1993.

[9] Bilanin, A. J., "Scaling Laws for Testing Airfoils under Heavy Rainfall," *Journal of Aircraft*, Vol. 24, No. 1, Jan. 1987, pp. 31-37.

[10] Markowitz, A. M., "Raindrop Size Distribution Expression," *Journal of Applied Meteorology,* Vol. 15, 1976, pp. 1029-1031.

[11] Dunham, R. E. Jr., "The Potential Influence of Rain on Airfoil Performance," von Karman Institute for Fluid Dynamics, 1987.

[12] Haines, P. A. and Luers, J. K., "Aerodynamic Penalties of Heavy Rain on Landing Aircraft," *Journal of Aircraft*, Vol. 20, No. 2, February 1983, pp. 111-119.

[13] Fluent's User Guide.

[14] Gong, D. T., Personal communication.

[15] Abbot, I. H. and von Doenhoff, A. E., *Theory of Wing Section: Including a Summary of Airfoil Data,* Dover Publication, New York, 1959.

[16] Thompson, B. E., Jang, J., and Dion, J. L., "Wing Performance in Moderate Rain," *Journal of Aircraft*, Vol. 32, No. 5, Sept.-Oct. 1995, pp. 1034-1039.

[17] Hasting, E. C. Jr. and Manuel, G. S., "Scale-Model Tests of Airfoils in Simulated Heavy Rain," *Journal of Aircraft*, Vol. 22, No. 6, June 1985, pp. 536-540.

Copyright Statement